Supplementary material
DUDF: Differentiable Unsigned Distance Fields with Hyperbolic Scaling

Miguel Fainstein[1] miguelon.f98@gmail.com
Viviana Siless[1] viviana.siless@utdt.edu
Emmanuel Iarussi[1,2] emmanuel.iarussi@utdt.edu
[1]Universidad Torcuato Di Tella, [2]CONICET

1. Differentiability analysis

Given a smooth surface $\mathcal{S}$, we want to study the differentiability of function:

$$t_{\mathcal{S}}(\mathbf{x}) = d_{\mathcal{S}}(\mathbf{x}) \tanh(\alpha d_{\mathcal{S}}(\mathbf{x})). \tag{1}$$

Notice that function $d_{\mathcal{S}}$ is differentiable almost everywhere outside the surface, hence $t_{\mathcal{S}}$ is trivially differentiable at such points and its gradient is given by:

$$\nabla t_{\mathcal{S}}(\mathbf{x}) = \nabla d_{\mathcal{S}}(\mathbf{x}) \phi(\mathbf{x}), \tag{2}$$

with $\phi(\mathbf{x}) = \tanh(\alpha d_{\mathcal{S}}(\mathbf{x})) + \alpha d_{\mathcal{S}}(\mathbf{x})(1 - \tanh^2(\alpha d_{\mathcal{S}}(\mathbf{x})))$. However, at the isosurface $d_{\mathcal{S}}$ is not differentiable. To show $t_{\mathcal{S}}$ differentiable at $\mathbf{s} \in \mathcal{S}$, we consider the partial derivatives expressed by the limit:

$$\lim_{h \to 0} \frac{t_{\mathcal{S}}(\mathbf{s} + \mathbf{e}_i h) - t_{\mathcal{S}}(\mathbf{s})}{h} = \lim_{h \to 0} \frac{t_{\mathcal{S}}(\mathbf{s} + \mathbf{e}_i h)}{h}, \tag{3}$$

where $\mathbf{e}_i$ is the i-th canonical vector. It follows that $d_{\mathcal{S}}(\mathbf{s} + \mathbf{e}_i h) \leq |h|$. Considering that function $\tanh$ is monotonically increasing, then:

$$\left| \frac{t_{\mathcal{S}}(\mathbf{s} + \mathbf{e}_i h)}{h} \right| \leq \left| \frac{|h| \tanh(\alpha |h|)}{h} \right| = |\tanh(\alpha |h|)| \xrightarrow{h \to 0} 0. \tag{4}$$

Hence, partial derivatives at the isosurface are null. To finish the proof, we show that the hyperplane defined by the partial derivatives at $\mathbf{s}$ correctly approximates the function $t_{\mathcal{S}}$, which is satisfied if the following limit approaches 0:

$$\lim_{\mathbf{x} \to \mathbf{s}} \frac{|t_{\mathcal{S}}(\mathbf{x}) - t_{\mathcal{S}}(\mathbf{s}) - \nabla t_{\mathcal{S}}(\mathbf{s}) \cdot (\mathbf{x} - \mathbf{s})|}{\|\mathbf{x} - \mathbf{s}\|} = \lim_{\mathbf{x} \to \mathbf{s}} \frac{|t_{\mathcal{S}}(\mathbf{x})|}{\|\mathbf{x} - \mathbf{s}\|}. \tag{5}$$

Similar to the partial derivative calculation, we bound this limit considering that the distance of every point to the surface must always be smaller or equal to the euclidean distance between a point and some surface point, that is $d_{\mathcal{S}}(\mathbf{x}) \leq \|\mathbf{x} - \mathbf{s}\|$ for every $\mathbf{s} \in \mathcal{S}$. Using this fact in Eq. 5:

$$\frac{|t_{\mathcal{S}}(\mathbf{x})|}{\|\mathbf{x} - \mathbf{s}\|} \leq \frac{\|\mathbf{x} - \mathbf{s}\| \, |\tanh(\alpha d_{\mathcal{S}}(\mathbf{x}))|}{\|\mathbf{x} - \mathbf{s}\|} = |\tanh(\alpha d_{\mathcal{S}}(\mathbf{x}))| \xrightarrow{\mathbf{x} \to \mathbf{s}} 0, \tag{6}$$

concluding that function $t_{\mathcal{S}}$ is differentiable at the isosurface.

2. Gradient norm

Based on the results from Sec. 1, at points outside the isosurface where $d_{\mathcal{S}}$ is differentiable, the unsigned distance gradient norm is unitary: $\|\nabla d_{\mathcal{S}}(\mathbf{x})\| = 1$. This is a standard property of distance functions. Given that ϕ is always positive away from the isosurface, the norm of the gradient can be expressed as:

$$\|\nabla t_{\mathcal{S}}(\mathbf{x})\| = \|\nabla d_{\mathcal{S}}(\mathbf{x})\| \, |\phi(\mathbf{x})| = \phi(\mathbf{x}). \tag{7}$$

As previously discussed, at the isosurface the gradient $\nabla t_{\mathcal{S}}(\mathbf{s}) = \mathbf{0}$, then its norm is null. These results explain the choice for the *Eikonal* problem and *Neumann* boundary condition expressed in the paper.

3. Extended ablation and results

As mentioned in the paper, we experimented with different values for parameter α (Tab. 1). As α gets larger, function $t_{\mathcal{S}}$ closely approximates $d_{\mathcal{S}}$, increasing the errors probably due to the non-differentiability at the isosurface. Smaller α values enlarge the quadratic strip near the isosurface, which is harder to supervise effectively and hinders the performance of MC.

We also show additional qualitative comparisons for three different experiments showcased in the paper. In Fig. 1 we demonstrate the effect of the maximum curvature field alignment loss on two reconstructed examples. In Fig. 2 we compare closed surface representations trained on the ShapeNet Cars data set [3] pre-processed by [8] to be closed. In Fig. 3 we show how our field's normal directions and principal curvatures are useful in the context of tracing rendering algorithms and light reflection models. Finally, in Fig. 4 we further compare the different reconstruction algorithms used throughout this work. All reconstructions were performed with the parameters reported in the paper (architecture, parameter count, loss weights, and training scheme).

α	L1CD ↓	L2CD ↓	NC ↓
1×10^0	10.7	0.038	0.094
1×10^1	9.23	**0.025**	0.033
1×10^2	**9.14**	0.027	**0.020**
1×10^3	9.52	0.038	0.023
1×10^4	9.69	0.029	0.028

Table 1. L1, L2 Chamfer distance and Normal Consistency (NC) metrics for different values of parameter α.

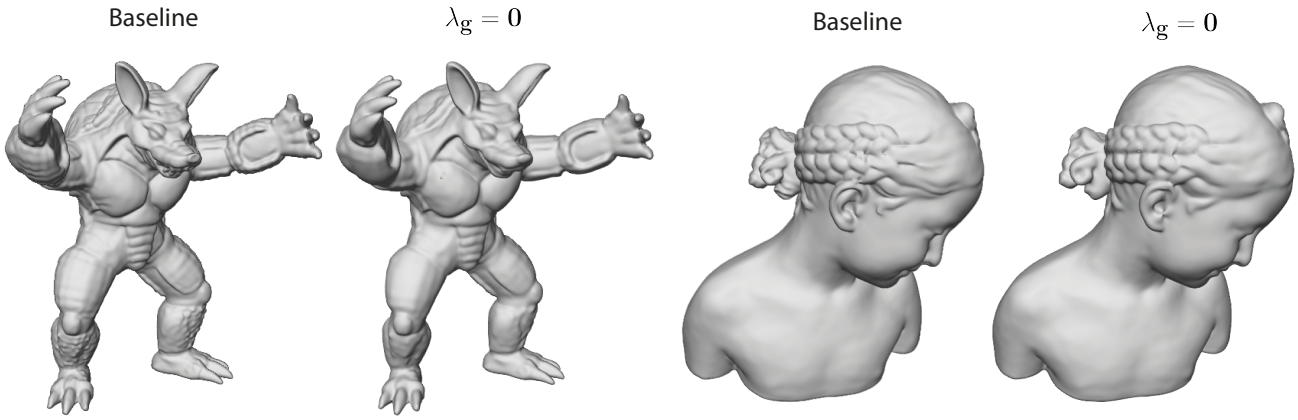

Figure 1. Ablation study. The first column shows the reconstruction of the network trained with the full loss. The second column shows the reconstruction without the maximum curvature field alignment term, resulting in less detail at high curvature regions such as Armadillo's mouth and Bimba's hair bun.

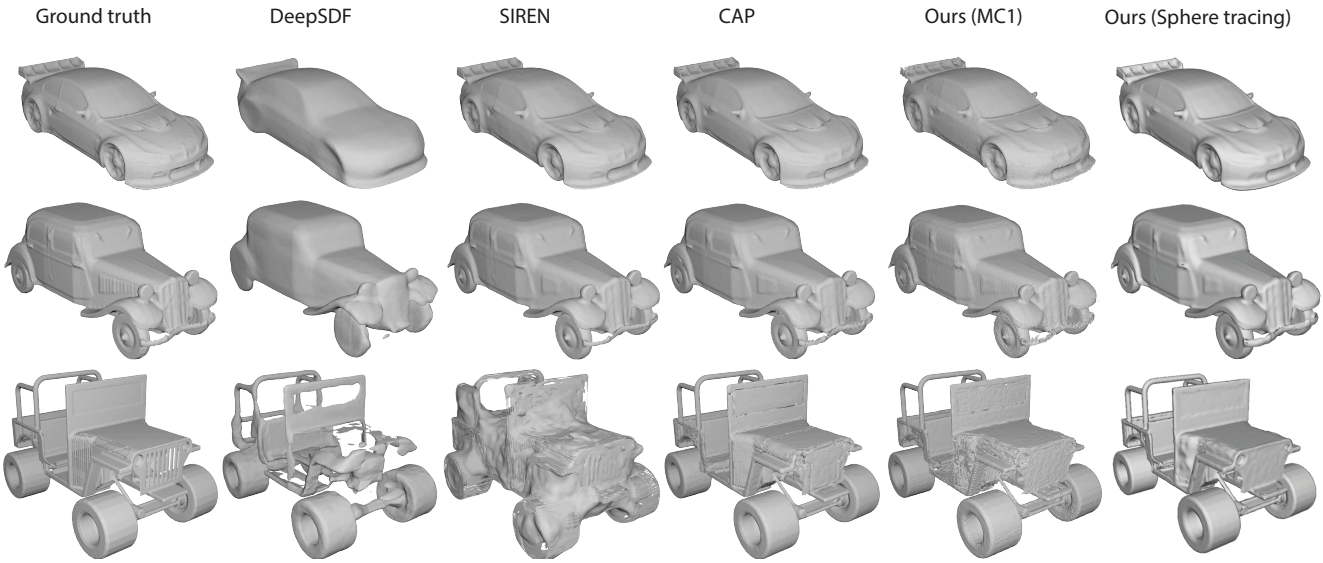

Figure 2. Reconstructions on closed [8] ShapeNet cars [3] for DeepSDF [5], SIREN [6], CAP-UDF [9] and DUDF. We additionally show sphere tracing renderings of our learned fields without the marching cubes reconstruction step.

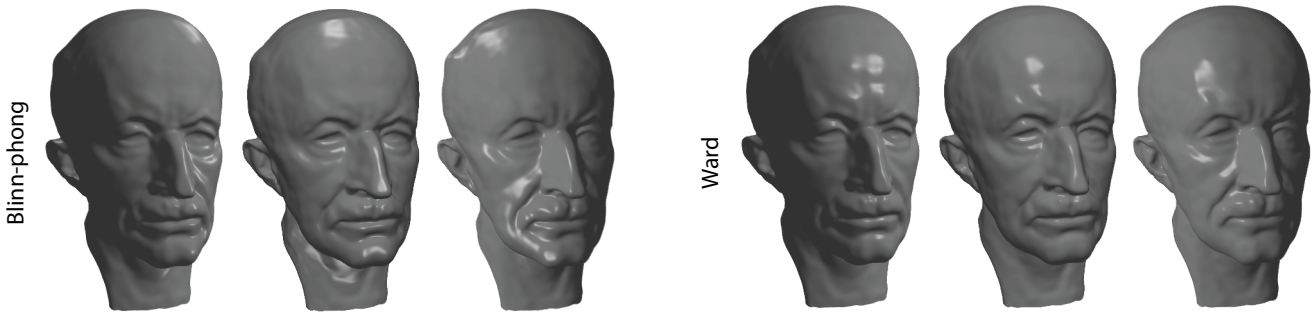

Figure 3. Sphere tracing renderings of an open surface (Max Planck model is open at the bottom) under three different light sources. We used surface normals for the Blinn-phong reflectance model [2]. For the Ward reflectance model [7] we used both, normals and principal curvature directions computed from DUDF's differentiable fields.

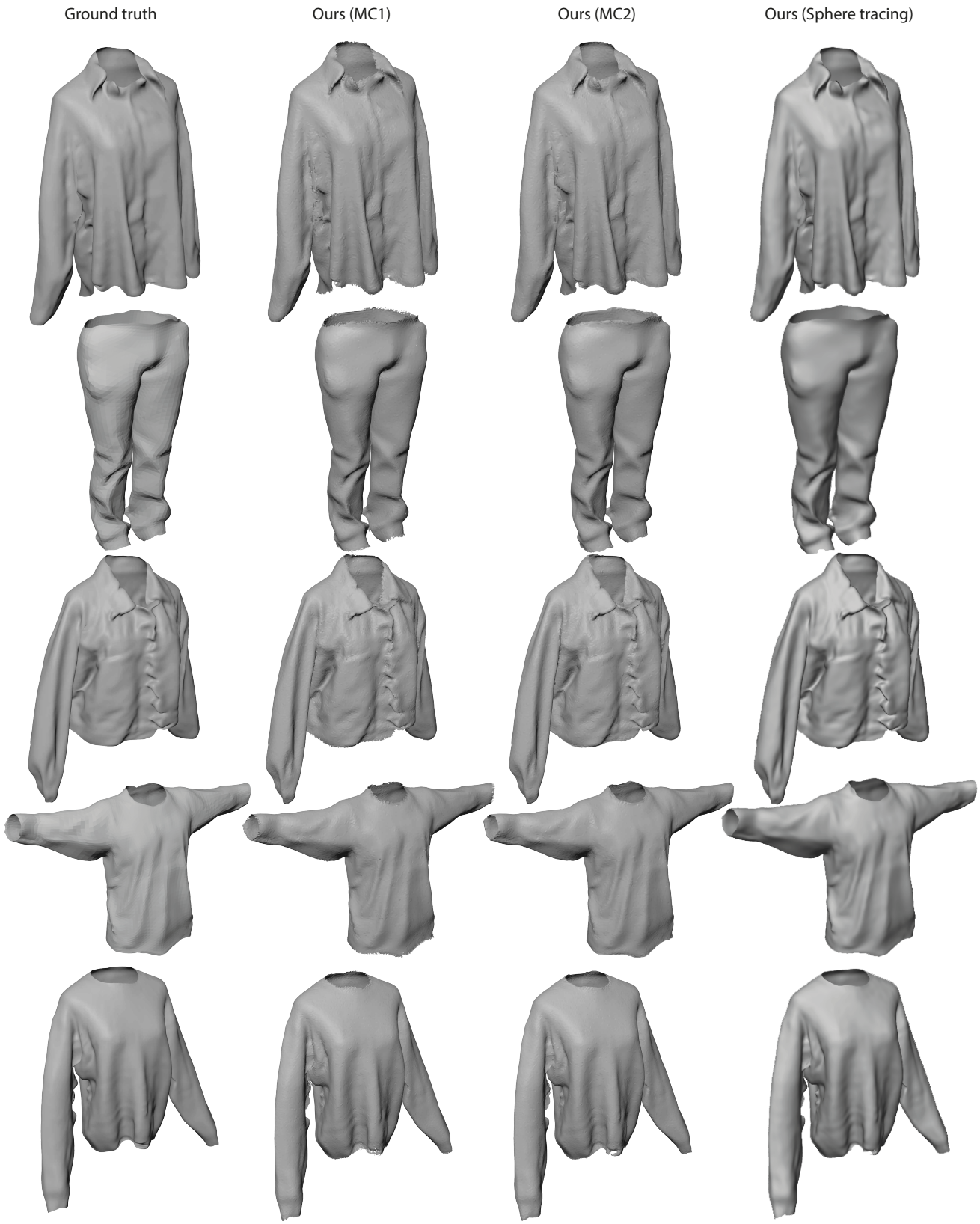

Figure 4. Reconstructions on DeepFashion [10] and Multi-garment [1] data sets for the three different reconstruction methods explored in our work: MC1 [9], MC2 [4], and sphere tracing.

References

[1] Bharat Lal Bhatnagar, Garvita Tiwari, Christian Theobalt, and Gerard Pons-Moll. Multi-garment net: Learning to dress 3d people from images. In *IEEE International Conference on Computer Vision (ICCV)*. IEEE, oct 2019. 3

[2] James F. Blinn. Models of light reflection for computer synthesized pictures. page 192–198, 1977. 2

[3] Angel X Chang, Thomas Funkhouser, Leonidas Guibas, Pat Hanrahan, Qixing Huang, Zimo Li, Silvio Savarese, Manolis Savva, Shuran Song, Hao Su, et al. Shapenet: An information-rich 3d model repository. *arXiv preprint arXiv:1512.03012*, 2015. 1, 2

[4] Benoit Guillard, Federico Stella, and Pascal Fua. Meshudf: Fast and differentiable meshing of unsigned distance field networks, 2022. 3

[5] Jeong Joon Park, Peter Florence, Julian Straub, Richard Newcombe, and Steven Lovegrove. Deepsdf: Learning continuous signed distance functions for shape representation. In *Proceedings of the IEEE/CVF conference on computer vision and pattern recognition*, pages 165–174, 2019. 2

[6] Vincent Sitzmann, Julien Martel, Alexander Bergman, David Lindell, and Gordon Wetzstein. Implicit neural representations with periodic activation functions. *Advances in neural information processing systems*, 33:7462–7473, 2020. 2

[7] Gregory J. Ward. Measuring and modeling anisotropic reflection. 26(2):265–272, 1992. 2

[8] Qiangeng Xu, Weiyue Wang, Duygu Ceylan, Radomir Mech, and Ulrich Neumann. Disn: Deep implicit surface network for high-quality single-view 3d reconstruction. *CoRR*, abs/1905.10711, 2019. 1, 2

[9] Junsheng Zhou, Baorui Ma, Yu-Shen Liu, Yi Fang, and Zhizhong Han. Learning consistency-aware unsigned distance functions progressively from raw point clouds. In *Advances in Neural Information Processing Systems (NeurIPS)*, 2022. 2, 3

[10] Heming Zhu, Yu Cao, Hang Jin, Weikai Chen, Dong Du, Zhangye Wang, Shuguang Cui, and Xiaoguang Han. Deep fashion3d: A dataset and benchmark for 3d garment reconstruction from single images. *CoRR*, 2020. 3